The Astrophysical Journal, 705:L217–L222, 2009 November 10 doi:10.1088/0004-637X/705/2/L217

EXCITATION OF KINK WAVES DUE TO SMALL-SCALE MAGNETIC RECONNECTION IN THE CHROMOSPHERE?

Jiansen He[1], Eckart Marsch[1], Chuanyi Tu[2], and Hui Tian[1,2]
[1] Max-Planck-Institut für Sonnensystemforschung, 37191 Katlenburg-Lindau, Germany; jshept@gmail.com
[2] Department of Geophysics, Peking University, Beijing, 100871, China
Received 2009 July 27; accepted 2009 October 12; published 2009 October 26

ABSTRACT

The kink wave, which has often been observed in coronal loops, is considered as a possibly important energy source contributing to coronal heating. However, its generation has not yet been observed. Here, we report the first observation of kink-wave excitation caused by magnetic reconnection as inferred from Solar Optical Telescope measurements made in the Ca II line. We observed transverse-displacement oscillations on a spicule which propagated upwardly along the spicule trace and originated from the cusp of an inverted Y-shaped structure, where apparently magnetic reconnection occurred. Such transverse oscillation of an individual spicule is interpreted by us to be the signature of a kink wave that was excited by magnetic reconnection. We present the height variations of the velocity amplitude, δv, and the phase speed, C_k, of the kink wave, starting from its source region. The kink wave is found to steepen with height and to evolve into a nonlinear state with a large relative disturbance, yielding a $(\delta v/C_k)$ of 0.21 at 5.5 Mm. This nonlinear kink wave seems to be damped in velocity amplitude beyond 5.5 Mm, which may result from the conversion of transverse-fluctuation energy to longitudinal-motion energy required to sustain the spicule. We also estimate the energy flux density carried by the kink wave, and in spite of its attenuation in the transition region conclude it to be sufficient for heating the quiet corona. Our findings shed new light on future modeling of coronal heating and solar wind acceleration involving magnetic reconnection in the chromosphere.

Key words: Sun: activity – Sun: chromosphere – Sun: magnetic fields

1. INTRODUCTION

The heating of the upper chromosphere as well as the lower corona remains unexplained and an unsolved problem in solar physics. Dissipation of magnetohydrodynamic (MHD) waves is a promising mechanism to solve the heating problem (Roberts 2004). The kink wave belongs to the class of fast magnetoacoustic waves, and is a kind of body wave that flexes a magnetic flux tube in a collective fluid mode. Several dissipation mechanisms for the kink wave have been suggested. Enhanced viscous dissipation of the localized Alfvén wave in a global kink loop is one possible mechanism (Ofman et al. 1994; Nakariakov et al. 1999). Phase mixing of Alfvén waves in the globally kinked loop is an alternative mechanism (Ofman & Aschwanden 2002). The energy transfer of the propagating kink wave to longitudinal oscillation was studied by Hasan et al. (2003), whereby the further dissipation occurred via shock heating. The propagating kink wave tends to be transformed to an Alfvén wave as it travels upwardly along the expanding flux tube into a more uniform medium (Cranmer et al. 2007). The Alfvén wave is generally believed to play a crucial role in the heating of coronal holes and acceleration of the fast solar wind in wave-driven wind models (Tu & Marsch 1997; Marsch & Tu 1997; He et al. 2008).

The kink wave has often been observed in the corona since the *Solar and Heliospheric Observatory* (*SOHO*) and *Transition Region and Coronal Explorer* (*TRACE*) missions (Nakariakov & Verwichte 2005) began operation. A standing fast magnetoacoustic kink wave was identified on coronal loops on the basis of *TRACE* observations, revealing transverse oscillatory displacements of coronal loops (Aschwanden et al. 1999; Nakariakov et al. 1999; Wang & Solanki 2004). The propagating kink wave was found to exist on a supra-arcade above a post-flare-loop arcade (Verwichte et al. 2005). However, in the chromosphere the kink wave has rarely been studied. Spicules, which appear in a periodicity of ∼5 minutes (Xia et al. 2005), can be used for the kink wave analysis. The kink wave signature was initially inferred from an observation of spatial periodicity in the Doppler velocity of Hα on a spicule (Kukhianidze et al. 2006). On the other hand, numerous oscillating spicules are considered as signals of ubiquitous Alfvén waves in the chromosphere (De Pontieu et al. 2007; He et al. 2009). The debate on the nature of these transverse spicule oscillations is not conclusive, since the expected oscillations of magnetic field lines in the interspicule space still remain unresolved.

The creation of a kink wave has not yet been observed directly. A flare event is often found to be associated with the standing kink wave, and is speculated to be a coronal trigger source for the kink wave (Aschwanden et al. 1999; Nakariakov et al. 1999). The kink wave propagating through the chromosphere into the corona is suggested in theory to be excited by the footpoint oscillation of flux tubes buffeted by side granules (Hasan et al. 2003). However, the direct connection between footpoint oscillation and kink wave has not been presented. On the other hand, small-scale magnetic reconnection at the junction of the magnetic network is supposed to generate the Alfvén waves required for coronal heating and solar wind acceleration (Axford & McKenzie 1992).

In this Letter, we show the generation of kink waves due to chromospheric small-scale magnetic reconnection, by using Solar Optical Telescope (SOT) observations (Tsuneta et al. 2008) in the Ca II H-line. The kink wave, which is identified by the transverse-displacement oscillation of the spicule trace, is found to propagate upwardly from the reconnection site. The evolution of the kink wave during its propagation, which covers the excitation, steepening, and attenuation, will be investigated. Moreover, the energy flux density carried by the kink wave is estimated on the basis of the observed phase speed and velocity

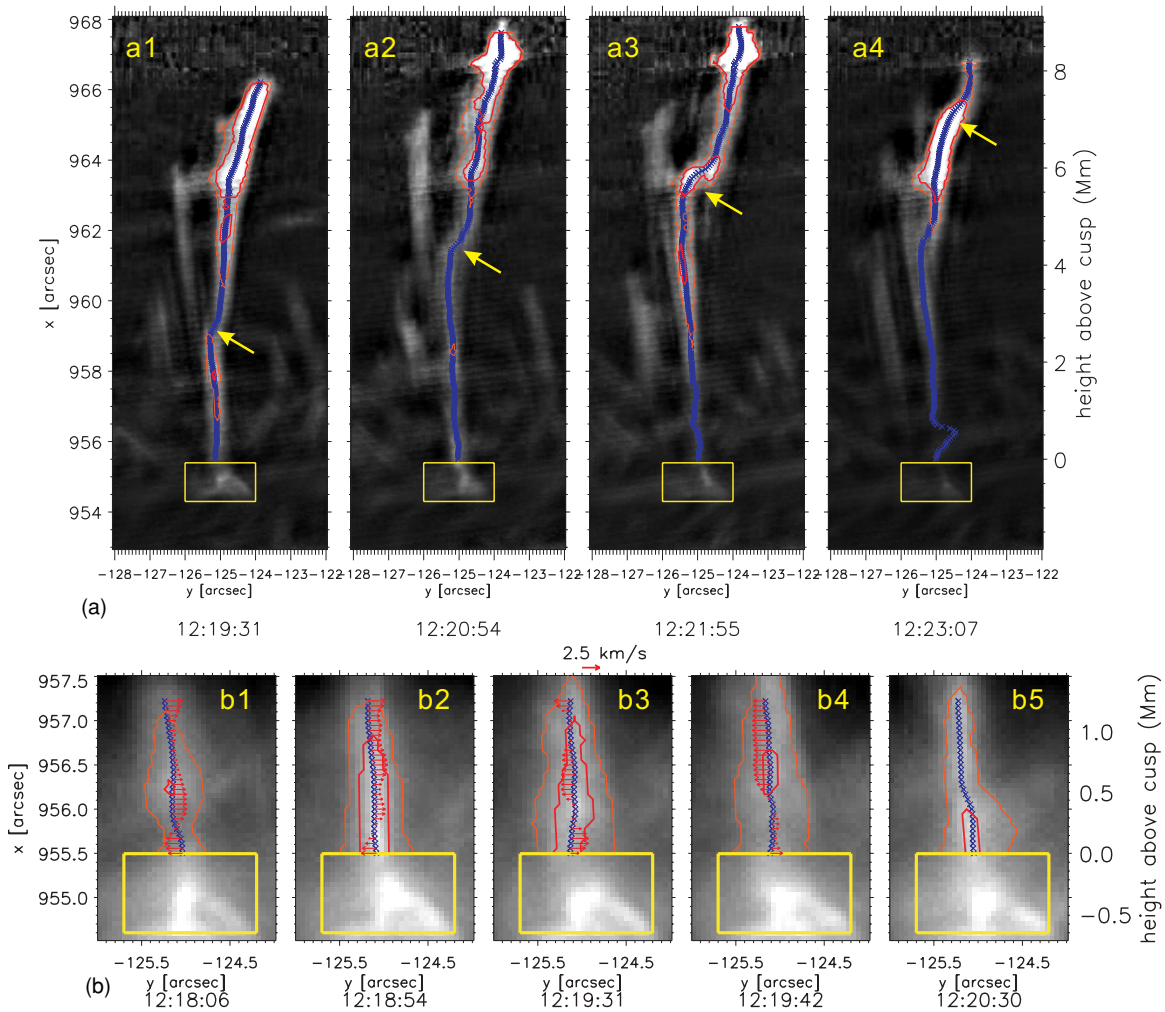

Figure 1. (a) Upward propagation of the transverse displacement, as marked with a yellow arrow in each panel, along the spicule trace. The red and brown contours surround the areas with intensities in the top 20% and top 40% of the image, respectively. The vertical coordinates on the right are the heights, with the origin being set at the cusp position ($x = 955\farcs5$). This height definition is also adopted in the following figures. (b) Transverse oscillations at the lower section of the spicule trace are shown for a time period ranging from pre-surge through surge to post-surge, with panel (b2) for the surge phase. Yellow box, red and brown contours have the same meaning as panels in (a). Four arrays of red arrows in panels (b1), (b2), (b3), and (b4) represent the oscillations from positions in the current panel toward the positions in the next panel, respectively.

amplitude, and is found to be comparable with the value required for coronal heating or solar wind acceleration in an individual plasma flow channel defined by a magnetic flux tube.

2. DATA REDUCTION

We used the data set obtained from SOT observations on 2007 January 14 in the Ca II H (3968 Å) line. During this time period, SOT was looking at the west limb with a cadence alternating between 11 s and 13 s. The spatial pixel size is $0\farcs054$.

We adopted the procedure "fg_prep.pro" available in Solar Software (SWW) to reduce the data and clean the images by removing the dark current and other camera artifacts. The correlation tracker system on SOT is used onboard satellite to remove most of the jitter between images (Shimizu et al. 2008). The slow pointing drift has a tiny influence on the image sequence, since this drift is less than $0\farcs2$ within 10 minutes. Like in the data analysis in He et al. (2009), here we also applied the normal radial gradient filtering (NRGF; Morgan et al. 2006) method to the images for the purpose of enhancing the visibility of structure dynamics off the solar limb, and then used the unsharp mask technique (Koutchmy & Koutchmy 1989) to eliminate the diffuse radiation intensity and to highlight the spicule trace in the off-limb region.

3. RESULTS AND ANALYSES

3.1. Dynamics of Spicule Trace Above a Reconnection Site

The event discussed here has been identified to be associated with small-scale magnetic reconnection, inferred from the observation of a jet launched from the inverted Y-shaped emission structure (Shibata et al. 2007). However, the wave excitation and propagation were not presented in that paper, as they become visible only after applying the unsharp-mask method to the image sequence.

The four panels in Figure 1(a) illustrate the spicule-trace dynamics. The spicule trace is shown as a strand of blue asterisks, the position of which is calculated by using a method presented by He et al. (2009). At the foot of the spicule, there is an inverted Y-shaped structure surrounded by a yellow box where magnetic reconnection was occurring and a jet was launched consequently (Shibata et al. 2007). The transverse-displacement oscillation of the spicule trace marked by a yellow arrow was moving upward in course of time. The transverse

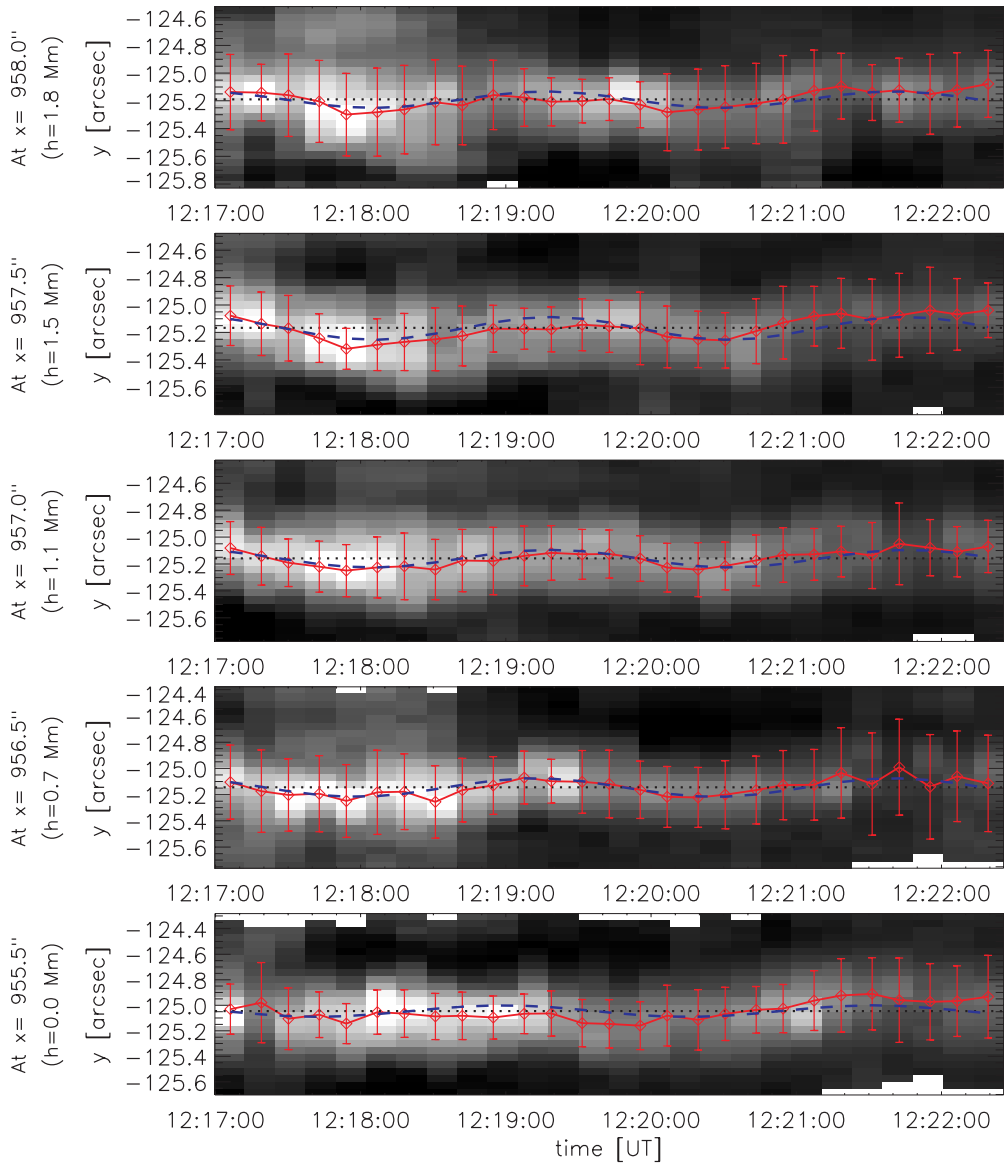

Figure 2. Diagrams of the transverse displacement vs. time for the Ca II intensity across the spicule at the lower section of spicule trace. The transverse displacement profile at each height is plotted as a red line with a strand of red diamonds. The half length of each vertical bar represents a σ width, which is defined in the text. The blue dashed line in each panel is the sine-fitting result for the transverse displacement profile. The black-dotted line is placed at the average position.

oscillation in the X-ray jet was suggested to be a coronal Alfvén wave (Cirtain et al. 2007). However, the spicule oscillation discussed here appeared to be isolated and did not have a connection with the ambient spicules. Therefore, we suggest that this upward propagating transverse oscillation may be related to kink-wave-like plasma and field activity.

The five panels of Figure 1(b) illustrate the spicule-trace dynamics at its root section. The spicule trace began to shake when a surge took place, apparently due to intermittent magnetic reconnection underneath. The spicule trace consequently oscillated in the post-surge period, and then recovered close to the pre-surge state after a period of oscillation. Therefore, we have observed the trigger of a kink wave caused by small-scale magnetic reconnection.

3.2. Transverse-displacement Oscillations on the Spicule

To study in more details the evolution of the kink wave during its propagation, we analyzed the transverse-displacement oscillations at various heights on the spicule trace. Figure 2 shows the transverse-displacement profiles at a lower section of the spicule trace. Red diamonds represent the center of spicule trace, while red vertical bars are used to show the 2σ width of the spicule trace. Here, we define the σ width as the square root of the variance for the intensity profile across the spicule. It can be seen in Figure 2 that the two side edges at the σ width oscillate in a similar way with its trace center. The lowest panel of Figure 2 shows the transverse-displacement profile at the cusp position of the invertedY-shaped structure. It can be seen in Figure 2 that the displacement oscillation is weak at the excitation site, and then strengthens with a clear pattern of oscillation at greater heights. Two periods of transverse-displacement oscillations are identified in Figure 2 in the time range from 12:17:00 to 12:22:00 UT. The oscillating displacement profiles at various heights are shown as red lines in the various panels of Figure 2, and are fitted with a sine function. The fitting results are plotted as blue dashed lines in Figure 2. Such fitting is reliable since the related error is less than the standard deviation of the oscillation profile.

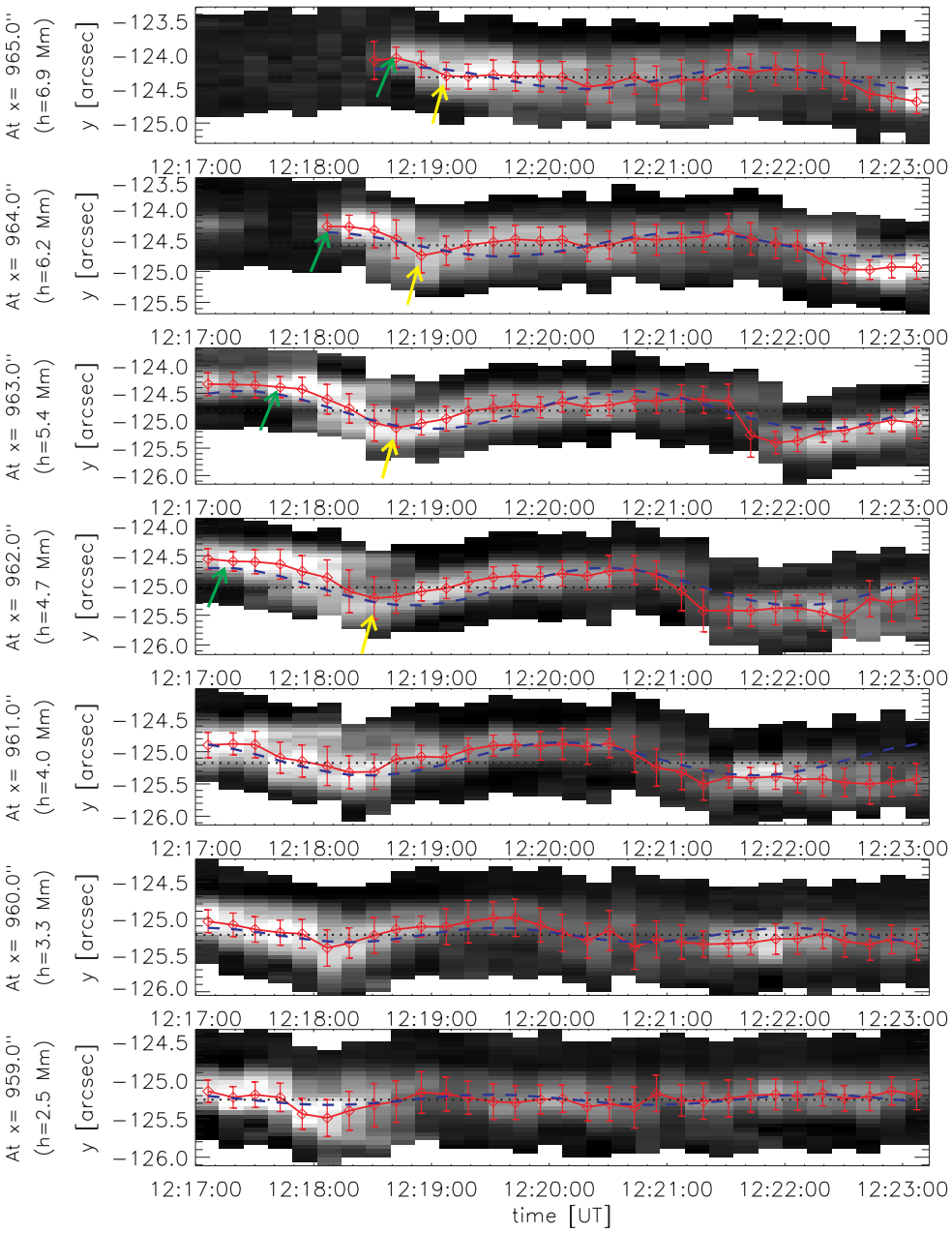

Figure 3. Transverse-displacement–time diagrams of the Ca II intensity across the spicule at the higher section of spicule trace. The transverse-displacement profile at each height is plotted as a red line with a strand of red diamonds. Vertical bars are used to mark the σ width on two sides. The sine-fitting results are shown as blue dashed lines. The average position is marked with a black dotted line. The yellow arrows represent the propagation of the transverse-displacement oscillation, and the green arrows denote the motion of the jet head.

Figure 3 illustrates the further evolution of this transverse-displacement oscillation at higher sections of the spicule trace. The blue dashed lines in the various panels of Figure 3 represent the sine-fitting results for the oscillation profiles obtained at different heights. It can clearly be seen that the displacement amplitude steadily increases up to the height of 5.4 Mm, beyond which it weakens again. Moreover, the oscillation phase is found to travel upward with time. Two bright patches in intensity, which are present in most panels, indicate the transits of two jets at various heights. In the two top panels of Figure 3, the intensity dimming above 6 Mm before 12:18:00 UT and strong brightening afterwards are caused by the extension of the spicule jet, which reaches higher than the pre-existing spicule would have normally done without the kink wave launched by magnetic reconnection.

Note that the transverse oscillation is not a passive disturbance advected along with the jet. The transverse oscillation (the yellow arrow in Figure 3) propagated faster than the jet head (the green arrow in Figure 3) at greater heights, where the jet plasma slowed down due to gravity. In magnetic reconnection theory, the phase speed of the transverse wave approximates the Alfvén speed (Takeuchi & Shibata 2001), and the plasma accelerated due to magnetic field relaxation will also approach the Alfvén speed (Birn & Priest 2007), and therefore the transverse wave and plasma will travel with a similar speed at some height where the plasma has its maximum speed. On the other hand, if the plasma flows without magnetic field relaxation as the driver, the wave will propagate relative to the flowing plasma, and the resulting phase speed in the solar inertial frame then is the sum of the flow speed and the phase speed in the plasma frame.

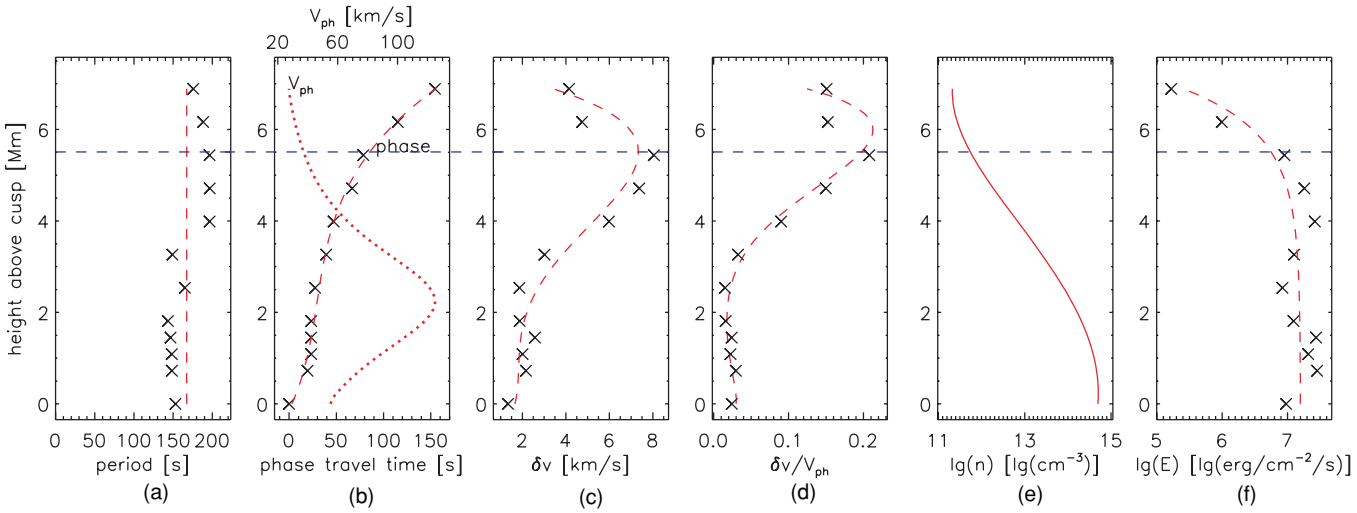

Figure 4. Height variation of parameters for the kink wave. The symbol "×" in the panels represents the parameter values at various heights, which are obtained by fitting the oscillation profiles with a sine function. (a) The periods for transverse oscillation at various heights are plotted as "×"s. The averaged period is marked with a red vertical line. (b) The phase travel times are plotted as "×"s, which are fitted with a polynomial function and plotted as a red dashed line. The phase speed profile is plotted as a red dotted line. (c) The velocity amplitudes are plotted as "×"s, and the polynomial-fitting result is given by the red dashed line. (d) The height variation of relative disturbance is plotted as a red dashed line. (e) The assumed number density profile, which has appropriate values both for the low chromosphere and the transition region, is plotted as a red solid line. (f) The profile of energy flux density carried by the kink wave, which is scaled to $h = 5.5$ Mm, is plotted as "×"s. The fitting result is shown as a red dashed line.

3.3. Height Variation of Parameters for the Kink Wave

Figure 4 shows the height variation of some parameters for the kink wave, i.e., period, phase travel time, phase speed, velocity amplitude, and relative disturbance, which are obtained from sine-fitting result. The periods at various heights are shown as "×"s in Figure 4(a). The average period is estimated to be 167 s.

A height–time diagram of the wave phase is shown in Figure 4(b), with the polynomial-fit result being plotted as the red dashed line which may be called phase–travel-time profile. The phase speed variation is further derived from the first-order temporal derivative of this profile. It is plotted as a red dotted line in Figure 4(b). The phase speed starts from 60 km s^{-1} at the cusp, increases to a maximum value of 125 km s^{-1} at 2.25 Mm, and then decreases to 25 km s^{-1} at 6.9 Mm. This height variation of the phase speed may be due to the changes of the magnetized plasma environment. The increase in phase speed at the beginning is probably due to the enhancement of the magnetic field intensity away from the reconnection site, at which the magnetic field intensity is close to zero. The decrease in phase speed at greater heights is supposed to be the result of a mass–density enhancement, due to a lifting-up of the transition region plasma.

According to van Doorsselaere et al. (2008), the kink wave can be considered as incompressible from an observational point of view, suggesting an approximation of the kink-wave phase speed by the Alfvén speed. The Alfvén speed in the low solar atmosphere is assumed to be on the order of 45 to 200 km s^{-1} (De Pontieu et al. 2007), but it can also be as small as 20 km s^{-1} for denser plasma in the chromosphere (Shibata et al. 2007). Therefore, the phase-speed range obtained here is compatible with values predicted for a kink wave in the chromosphere. The phase speed of 25 km s^{-1} at 6.9 Mm is somewhat small in comparison with the Alfvén speed of 44 km s^{-1}, if we assume that $B = 10$ G and $n = 2.4 \times 10^{11}$ cm^{-3} in the upper chromosphere. In a steady stratified solar atmosphere model, the Alfvén speed generally increases monotonously above the upper photosphere, but in the real dynamic atmosphere discussed here, the Alfvén speed profile may deviate somewhat from such a model profile.

The height variation of the velocity amplitude is shown in Figure 4(c). It increases from 1.3 km s^{-1} at the cusp to 8.0 km s^{-1} at 5.4 Mm above the cusp, and weakens beyond 5.4 Mm. We have fitted its height variation with a polynomial and plotted the fitting result as a red dashed line. The relative disturbance ($\delta v/C_k$) is shown in Figure 4(d). Initially, it is 0.02 and then increases to 0.21 at 5.5 Mm. Such a large relative disturbance indicates the evolution of the kink wave toward nonlinearity. An attenuation of the velocity amplitude, as well as of the relative disturbance, is identified at greater heights. In numerical simulation, the kink wave was calculated to lose part of its energy in the chromosphere below the magnetic canopy, due to an energy transfer to longitudinal waves (Hasan et al. 2003). Similar nonlinear coupling between transverse and longitudinal oscillations has also been modeled for the Alfvén wave (Kudoh & Shibata 1999). In our case study, the extending longitudinal motion of the spicule plasma beyond 6 Mm is associated with an attenuation in the transverse velocity amplitude of the kink wave. Therefore, the transverse fluctuation of the kink wave in our case might be damped by delivering its energy to longitudinal fluctuations.

To estimate the energy flux density carried by the excited kink wave, we assume a typical number density profile plotted in Figure 4(e), which has a value of 0.6×10^{15} cm^{-3} for the spicule root in the solar chromosphere (Shibata et al. 2007) and a value of 2.4×10^{11} cm^{-3} for the spicule section in the transition region (Beckers 1968). Therefore, the energy flux density for the nearly incompressible kink wave, which is scaled to the height $h_0 = 5.5$ Mm, can be approximated as $\rho\delta v^2 C_k A/A_0$, where A/A_0 is the area ratio that is approximated by $B_0/B \simeq (C_k\sqrt{\rho})|_{h0}/(C_k\sqrt{\rho})|_h$, whereby a constant ratio of the density inside the spicule to outside is assumed along the height (van Doorsselaere et al. 2008). The energy flux densities at various heights are thus estimated and plotted as "×"s in Figure 4(f), the fitting result of which is plotted as a red

dashed line in that figure. It shows that the energy flux density keeps nearly constant at a value of $\sim 1.5 \times 10^7$ erg cm^2 s^{-1} from $h = 0$ Mm to $h = 4$ Mm, and then decreases to $\sim 0.25 \times 10^6$ erg cm^2 s^{-1} at $h = 7$ Mm.

4. SUMMARY AND DISCUSSION

We have for the first time presented the observation of a kink-wave excitation caused by small-scale magnetic reconnection in the solar chromosphere. The dynamics of the spicule trace becomes clearly visible after applying the NRGF and unsharp-mask methods to the image sequence. The kink wave is identified by the upward propagation of a transverse-displacement oscillation along the spicule trace. Moreover, this transverse oscillation appears to originate from the cusp position of an inverted Y-shaped magnetic structure, where a surge (jet launch) was taking place, indicating the occurrence of magnetic reconnection according to Shibata et al. (2007).

The characteristics of the kink wave along the spicule with height, i.e., its velocity amplitude, wave period, and phase speed, have been determined and investigated. This is the first time, according to our knowledge, that the steepening of a kink wave from small amplitude at the source region to the nonlinear state at greater height is observed. This enhanced amplitude was partly damped with greater altitude, and could be associated with the extending upward motion of the spicule plasma. Theoretical studies have predicted that nonlinear Alfvén wave can transfer part of the transverse oscillation energy to energy related to longitudinal motion, and thus lift up material in the transition region (Kudoh & Shibata 1999). The nonlinear energy conversion from the kink wave to a longitudinal wave in the chromosphere has been studied by Hasan et al. (2003). We suggest that future modeling of the nonlinear coupling between the kink wave and the longitudinal motion should be extended to the transition region and its effect on the upward motion of plasma should be studied.

The kink wave in our case is estimated to carry an initial energy flux density of 1.5×10^7 erg cm^{-2} s^{-1} in the low solar chromosphere. The energy flux density is estimated to decrease to 0.25×10^6 erg cm^{-2} s^{-1} in the transition region. Therefore, the energy flux density carried by the kink wave, despite its attenuation in the chromosphere and the transition region, still is sufficient for heating the quiet corona and/or driving the solar wind, which needs an energy input on the order of 10^6 erg cm^2 s^{-1} (Hansteen & Leer 1995). The present finding that a kink wave can be generated by small-scale magnetic reconnection suggests a new way of linking magnetic activity in the chromosphere with the heating of the solar corona. The presented data analysis suggests a kink wave is plausible, but not completely on solid ground, since we do not have simultaneous observations of plasma density and magnetic field. Further observations with more evidence may resolve the remaining uncertainty. Here, we have merely presented one case of a kink-wave-like phenomenon, but future statistical study is needed for fully revealing the kink-wave characteristics in the chromosphere.

Hinode is a Japanese mission developed and launched by ISAS/JAXA, with NAOJ as domestic partner and NASA and STFC (UK) as international partners. It is operated by these agencies in cooperation with ESA and NSC (Norway). SOT onboard *Hinode* was developed jointly by NAOJ, LMSAL, ISAS/JAXA, NASA, HAO, and MELCO. J.H. is supported by the post-doctor fellowship at MPS. C.T. is supported by the National Natural Science Foundation of China under Contract Nos. 40874090, 40931055, and 40891062.

REFERENCES

Aschwanden, M. J., Fletcher, L., Schrijver, C. J., & Alexander, D. 1999, ApJ, 520, 880
Axford, W. I., & McKenzie, J. F. 1992, in Proc. 3rd COSPAR Colloqium, Solar Wind Seven, ed. E. Marsch & R. Schwenn (Oxford: Pergamon), 1
Beckers, J. M. 1968, Sol. Phys., 3, 367
Birn, J., & Priest, E. R. 2007, in Reconnection of Magnetic Fields: Magnetohydrodynamics and Collisionless Theory and Observations, ed. J. Birn & E. R. Priest (Cambridge: Cambridge Univ. Press), 18
Cirtain, J. W., et al. 2007, Science, 318, 1580
Cranmer, S. R., van Ballegooijen, A. A., & Edgar, R. J. 2007, ApJS, 171, 520
De Pontieu, B., et al. 2007, Science, 318, 1574
Hansteen, V. H., & Leer, E. 1995, J. Geophys. Res., 100, 21577
Hasan, S. S., Kalkofen, W., van Ballegooijen, A. A., & Ulmschneider, P. 2003, ApJ, 585, 1138
He, J.-S., Tu, C.-Y., & Marsch, E. 2008, Sol. Phys., 250, 147
He, J.-S., Tu, C.-Y., Marsch, E., Guo, L.-J., Yao, S., & Tian, H. 2009, A&A, 497, 525
Koutchmy, O., & Koutchmy, S. 1989, in Proc. 10th Sacramento Peak Summer Workshop, High Spatial Resolution Solar Observations, ed. O. van der Luhe (Sunspot, NM: NSO), 217
Kudoh, T., & Shibata, K. 1999, ApJ, 514, 493
Kukhianidze, V., Zaqarashvili, T. V., & Khutsishvili, E. 2006, A&A, 449, L35
Marsch, E., & Tu, C.-Y. 1997, Sol. Phys., 176, 87
Morgan, H., Habbal, S. R., & Woo, R. 2006, Sol. Phys., 236, 263
Nakariakov, V. M., Ofman, L., Deluca, E. E., Roberts, B., & Davila, J. M. 1999, Science, 285, 862
Nakariakov, V. M., & Verwichte, E. 2005, Living Rev. Sol. Phys., 2, 3
Ofman, L., & Aschwanden, M. J. 2002, ApJ, 576, L153
Ofman, L., Davila, J. M., & Steinolfson, R. S. 1994, ApJ, 421, 360
Roberts, B. 2004, in Proc. *SOHO*-13, Waves, Oscillations and Small-Scale Transients Events in the Solar Atmosphere: Joint View from *SOHO* and *TRACE*, ed. H. Lacoste (ESA SP-547; Noordwijk: ESA), 1
Shibata, K., et al. 2007, Science, 318, 1591
Shimizu, T., et al. 2008, Sol. Phys., 249, 221
Takeuchi, A., & Shibata, K. 2001, ApJ, 546, L73
Tsuneta, S., et al. 2008, Sol. Phys., 249, 167
Tu, C.-Y., & Marsch, E. 1997, Sol. Phys., 171, 363
van Doorsselaere, T., Nakariakov, V. M., & Verwichte, E. 2008, ApJ, 676, L73
Verwichte, E., Nakariakov, V. M., & Cooper, F. C. 2005, A&A, 430, L65
Wang, T. J., & Solanki, S. K. 2004, A&A, 421, L33
Xia, L. D., Popescu, M. D., Doyle, J. G., & Giannikakis, J. 2005, A&A, 438, 1115